Synthesis of Compliance Linkage Mechanism Based on Topology Optimization and Image Processing Techniques

Po Ting Lin, NTUST, Chyi-Yeu Lin, NTUST, and Tung-Yao Cheng, NTUST

***Abstract*—Compliance mechanisms have been used in the design of soft grippers or flexible mechanisms, whose mobilities came from the flexibility of their members rather than the rigid parts in the mechanisms. Compliance linkage mechanisms, that are composed of multiple straight linkages, are simple to manufacture and could be easily applied to the desired gripper designs. One way to synthesize the compliance linkage mechanisms is Topology Optimization (TO). TO methods have been well developed for structural and multidisciplinary designs in terms of finding the optimal objective functions subject to constraints of loading conditions and other design requirements. In practical uses, clear black-and-white optimal designs (i.e. structural design with nonfuzzy distribution of elemental members) are desired but may not be delivered at the end of the TO procedures. Therefore, many additional treatments such as regularization and filtering have been developed to produce black-and-white designs. Some of the said procedures were also found in the fields of computer vision and image processing. This paper presents a method to automatically generate linkage designs by applying image-processing techniques to TO designs. The presented post-processing procedure includes noise removal, pattern thinning, and automatic determination of linkage nodes linages. Several numerical examples were shown to demonstrate the presented methodology for automatic linkage designs.**

Index Terms—Compliance Linkage Mechanism, Topology Optimization, Image Processing, Gripper Design.

I. INTRODUCTION

TOPOLOGY Optimization (TO) methods have been developed for structural designs in various engineering applications such as aerospace, automobile, engineering, energy, civil engineering, etc. Starting from the year of 1904, Australian inventor George Michell [1] analytically solved the structural design problems to determine the optimal topologies of the structure under certain loading conditions and constraints. The concept of Topology Optimization (TO) has become one of the most important methods of synthesizing the structural layout and determining the optimal design parameters. Prager [2] derived analytical TO solutions based on Optimality Criteria (OC). Bendsøe and Kikuchi [3] developed Homogenization method to determine optimal density distributions in the chosen design domain with predefined degree-of-freedom and loading conditions. Recently, TO problems were often solved based on density-based approaches, such as Solid Isotropic Material with Penalization (SIMP) [4] that used a power-law interpolation model of material density. Manuel [5-8] compared the effects of different material interpolation models, include Rational Approximation of Material Properties (RAMP) [9], hyperbolic sine function [10], Krischer function [11], Maxwell-Hamilton model [12] and Effective Medium Theory (EMT) [13], to the TO of heat conduction designs. On the other hand, Sigmund [14] used TO to synthesize the compliance mechanisms based on given load conditions. Luo, et al. [15] developed a Level Set approach to find the optimal compliance mechanism designs under various settings of design parameters. In 2016, Jin and Zhang [16] developed a TO approach to design the planar compliance mechanisms that could be used for the applications of parallel manipulations. In 2019, Suh, et al. [17] presented the compliance planar linkage mechanisms that greatly reduced the number of variables in traditional TO approaches.

The common goal of the density-based TO methods is to find the optimal structural design based on the sensitivities of material densities. However, sensitivity analyses were not enough to produce manufacturable designs (i.e. black-and-white designs that have nonfuzzy distributions of elemental members) due to the nature of material continuity. Additional treatments would be needed to change the gray TO results to clear black-and-white designs. Modifications from gray to back-and-white designs have been done in the field of image processing. Charbonnier, et al. [18] had started to concept of edge-preserving smoothing using Tikhonov regularization in image processing. Both in image processing and TO, smoothing sometimes are necessary to remove the noises but not blurring the edges (i.e. pattern edges for image processing and structure edges for TO). Wang, et al. [19] investigated a series of diffusion (or smoothing) functions, which were developed in the image processing field, and utilized them as density filters in the TO processes. Some nonlinear diffusion functions [20] showed better edge-preserving performances than the linear regression of Tikhonov regularization. Sigmund [21] summarized a series of regularization schemes for production of black-and-white TO structures. The most common filters were mesh-independent and were developed based on the sensitivity around each element [14]. This sensitivity was computed by a weighted sum of the neighboring elements, or by the mean of the convolution product [22], which is very common in image processing [23,

This paper was first submitted in June 15, 2020. This work was supported by Center for Intelligent Robots at National Taiwan University of Science and Technology (NTUST), and Center for Cyber-Physical System Innovation, which is a Featured Areas Research Center in Higher Education Sprout Project of Ministry of Education (MOE), Taiwan (since 2018).

Po Ting Lin is the corresponding author of this paper. Dr. Lin is an Associate Professor in the Department of Mechanical Engineering at National Taiwan University of Science and Technology (NTUST), Taipei 10609, Taiwan (e-mail: potinglin@mail.ntust.edu.tw).

Chyi-Yeu Lin is a Distinguished Professor in the Department of Mechanical Engineering and the Director of Center for Intelligent Robots at National Taiwan University of Science and Technology (NTUST), Taipei 10609, Taiwan (e-mail: jerrylin@mail.ntust.edu.tw).

Tung-Yao Cheng was a MS student in the Department of Mechanical Engineering at National Taiwan University of Science and Technology (NTUST), Taipei 10609, Taiwan and graduated in July 2005 (e-mail: tungyao01@gmail.com).

24]. Zhang, et al. [25] used the convolution approach to control the length scales of beam members in the processes of TO. The material interpolation and sensitivity analysis of the TO process was based on SIMP [4]. Otsu thresholding [26] was used to convert a gray-valued design to a back-and-white design. Pattern thinning [27] was then used to obtain the one-pixel-wide skeleton of the TO design. The element density was then constrained in terms of its distance away from the skeleton in order to control the scale length of the TO design.

Instead of combining image processing techniques (such as filtering, regularization schemes, convolution operations, etc.) into the TO processes, Bremicker, et al. [28] directly used pattern thinning to find the skeleton of the topologically optimized structure and determined a truss design based on additional heuristic rules of node determination, linkage determination, redundant node removal, etc. Sigmund [21] showed promising results of black-and-white TO structures by directly applying image processing operations to the unfiltered TO results. Erosion operation eats away the boundaries of structures as well as the isolated noises; on the other hand, dilation operation grows the structural boundaries and seals the small holes. It was shown that the processes of repeating erosion and dilation were capable of generating black-and-white structural results. The advantage of the post-processing methods based on image processing techniques is that additional sensitivity analyses are no longer needed. Therefore, this paper presents a method to automatically generate linkage designs by applying image-processing techniques on TO designs.

II. Density-Based Topology Optimization

This paper started the TO design problem, where the structural compliance f of the design is minimized as shown below:

$$\begin{aligned} \underset{\mathbf{x}}{Min} \quad & f(\mathbf{x}) = \mathbf{U}^T\mathbf{K}(\mathbf{x})\mathbf{U} \\ s.t. \quad & \mathbf{K}(\mathbf{x})\mathbf{U} = \mathbf{F}(\mathbf{x}) \\ & \frac{\sum x_i v_i}{\sum v_i} \le V \\ & 0 \le x_i \le 1 \end{aligned} \tag{1}$$

where $\mathbf{x}$ is the vector of material densities, that vary from zero to one. $x_i = 0$ stands for an empty element while $x_i = 1$ represents the element is 100% filled with materials. $\mathbf{K}$ is the global stiffness material; $\mathbf{U}$ and $\mathbf{F}$ are vectors of degrees of freedom and loads, respectively. v_i is the elemental volume and V is the allowable volume fraction.

This paper uses SIMP [4] as the material interpolation model, as shown below:

$$E(x_i) = E_{\min} + x_i^p (E_0 - E_{\min}) \tag{2}$$

where the element modulus E_0 was scaled by the penalized variable and $p = 3$ was used as the penalty parameter in this paper. The sensitivity filter [29] in Eq. (3) was used to remove the checkerboard effect.

$$\frac{\partial \hat{f}}{\partial x_i} = \frac{\sum_j H_{ij} x_j \frac{\partial f}{\partial x_j}}{x_i \sum_j H_{ij}} \tag{3}$$

where the updated sensitivity $\partial \hat{f} / \partial x_i$ is computed based on a distance function H_{ij} that is given as:

$$H_{ij} = \max(0, R - dist(i, j)) \tag{4}$$

where $dist(i, j)$ stands for the distance between the i^{th} and j^{th} elements; R is a filter radius. Method of Moving Asymptotes (MMA) [30] was used to update the design variables.

The entire TO procedure can be seen in Fig. 1 (a). The process starts with the initial setup of boundary conditions, loading conditions, material properties and penalty parameters. For each iteration, Finite Element Analysis (FEA) is used to evaluate the objective function and constraint values as well as the sensitivity analysis. The filtering scheme shown in Eq. (3) is then used to remove checkerboard effects. This paper uses MMA to update the design variables. The final TO design will be determined until the convergence criterion is satisfied. The next section will introduce how to generate linkage designs based on post-processing of image processing techniques.

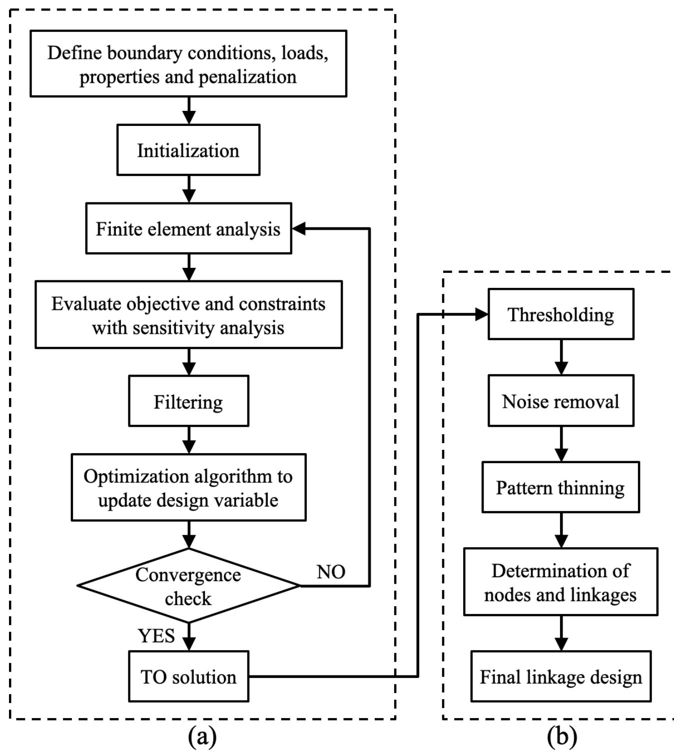

Fig. 1. Workflow of the automatic linkage design based on (a) TO [31-33] and (b) image processing techniques.

III. Linkage Design Based on Topology Optimization Results and Image processing Techniques

Compliance linage mechanisms have been developed for various applications, such as leg designs of walking robots [34, 35], compliance robot arm [36], compliance linkage gripper design [37], etc. This section shows a general solution process to automatically generate the linkage design using the proposed TO and image processing techniques, as mentioned in Fig. 1.

A. Removal of Noises and Holes

The first step is to obtain a completely black-and-white TO design using Otsu thresholding method [26]. Next, the isolated noises in the empty region, as shown in Fig. 2 (a), and the isolated holes in the material region, shown in Fig. 2 (b), should be removed in order to prevent formulation of unwanted skeleton patterns in the later procedures. A simple 3×3 mask is used to examine the entire design domain. An isolated noise can be identified when the kernel of the mask is 1 and the neighboring pixels all equal to 0. A second 3×3 mask is then used to find the isolated holes. When the kernel of the mask is 0 and the sum of the neighboring pixels is larger than 6, the kernel is either an isolated hole or a part of connected holes. The scanning processes using the aforementioned 3×3 masks can be performed multiple times for complete removal of isolated noises and holes. Once the isolated noises and holes were removed, the next procedure is to fill the structural notches, as shown in Fig. 2 (c). A third 3×3 mask is used to scan the entire design domain again. As the kernel of the mask is 0 and the sum of the neighboring pixels is larger than 4, the kernel is changed to 1.

B. Pattern Thinning

Pattern thinning [38] will be used to determine the skeleton of the TO design and identify the coordinates of nodes. However, the positioning of nodes will be difficult if the resolution of the TO design is low, as shown in Fig. 3 (a). Fig. 3 (b) shows the result of a resolution 9 times higher than the original design. The thinning method is based on a two-level procedure. Based on another 3×3 mask $I(i\pm1, j\pm1)$, the kernel $I(i,j)$ is to be removed (i.e. changed from 1 to 0) if the following conditions are all satisfied:

- Connectivity equals to 1;
- There are at least 2 but no more than 6 zero pixels in the mask;
- At least one pixel in $I(i,j+1)$, $I(i-1,j)$ and $I(i,j-1)$ is zero;
- At least one pixel in $I(i-1,j)$, $I(i+1,j)$ and $I(i,j-1)$ is zero.

The aforementioned pixels are removed at once after the first-level scanning. In the second level of scanning, the kernel is to be removed if the following conditions are all satisfied:

- At least one pixel in $I(i-1,j)$, $I(i,j+1)$ and $I(i+1,j)$ is zero;
- At least one pixel in $I(i,j+1)$, $I(i+1,j)$ and $I(i,j-1)$ is zero;
- At least one pixel in $I(i,j+1)$, $I(i-1,j)$ and $I(i,j-1)$ is zero;
- At least one pixel in $I(i-1,j)$, $I(i+1,j)$ and $I(i,j-1)$ is zero.

Fig. 4 shows the skeleton obtained by applying the said thinning procedure to Fig. 3 (b).

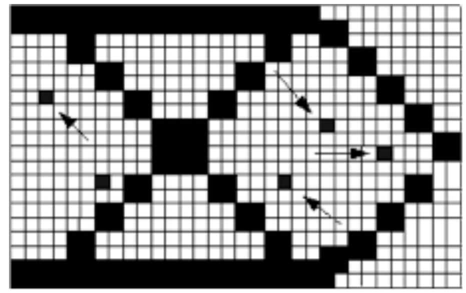

(a)

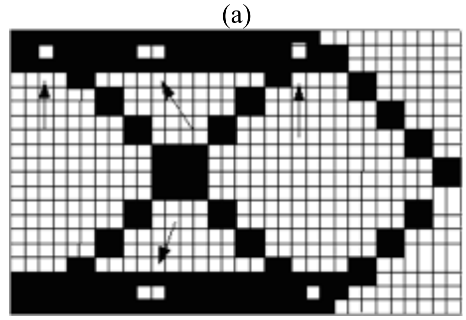

(b)

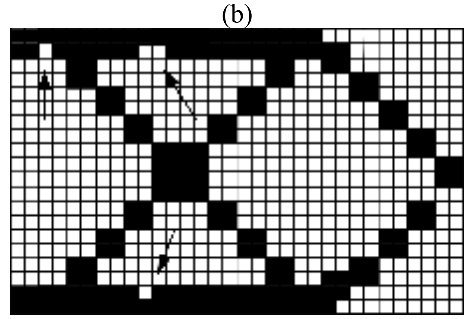

(c)

Fig. 2. TO designs with (a) isolated noises, (b) isolated holes and (c) structural notches.

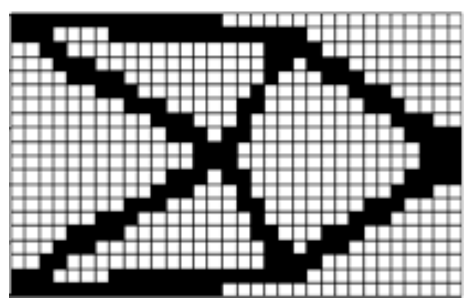

(a)

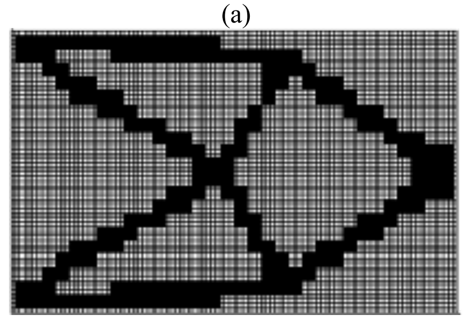

(b)

Fig. 3. TO designs with (a) the original and (b) increased resolutions.

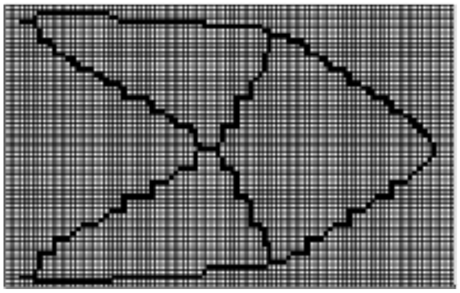

Fig. 4. Skeleton of the TO design using pattern thinning.

C. Determination of Nodes and Linkages

The following procedure of node identification is essential to achieve complete automation of linkage design. Using a different 3×3 mask, the kernel will be chosen as a candidate of linkage node if one of the following conditions is satisfied:

- If $I(i,j)=1$, sum of neighboring pixels ≥ 3, and $I(i-1,j+1)+I(i+1,j)+I(i-1,j-1)=3$;
- If $I(i,j)=1$, sum of neighboring pixels ≥ 3, and $I(i-1,j+1)+I(i+1,j)+I(i,j-1)=3$;
- If $I(i,j)=1$, sum of neighboring pixels ≥ 3, and $I(i-1,j)+I(i,j+1)+I(i+1,j)+I(i,j-1)=4$;
- If $I(i,j)=1$, sum of neighboring pixels ≥ 3, and $I(i-1,j+1)+I(i+1,j+1)+I(i+1,j-1)+I(i-1,j-1)=4$;
- If $I(i,j)=1$, sum of neighboring pixels $=3$, and $I(i-1,j+1)+I(i+1,j-1)+I(i-1,j-1)=3$;
- If $I(i,j)=1$, sum of neighboring pixels ≥ 3, and $I(i,j+1)+I(i+1,j)+I(i-1,j-1)=3$;
- If $I(i,j)=1$, sum of neighboring pixels ≥ 3, and $I(i-1,j)+I(i+1,j+1)+I(i,j-1)=3$.

Fig. 5 shows the obtained candidate of linkage nodes from the skeleton design shown in Fig. 4. Further corrections will be needed for the final generation of the linkage design. The first correction is to move the nodes that are located near the fixed boundary conditions to the said fixed points. The second step is to move the nodes that are located near the locations of loads to the said loafing points. Next, remove the redundant node points near the nodes (i.e. within a certain range with a reasonable radius) that were moved to the fixed and loading positions. If there are multiple candidates of nodes within a certain range of radius, choose the mean point of the said nodes as the new linkage node. Fig. 6 shows the final positions of the linkage nodes using the said procedures to correct the node arrangements in Fig. 5.

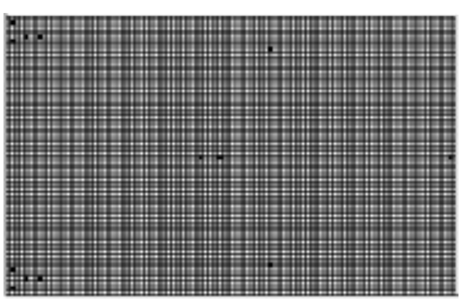

Fig. 5. Candidates of the linkage nodes.

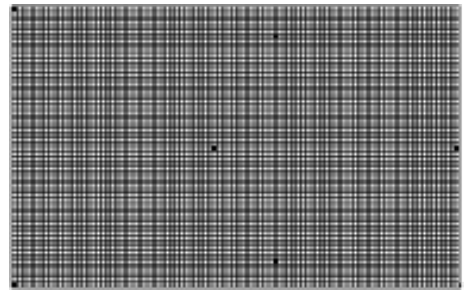

Fig. 6. Final positions of the linkage nodes after the presented correction procedures.

The final connectivity of the linkages are to be determined by comparing the skeleton design, shown in Fig. 4, and the node positions, shown in Fig. 6. A series of scanning procedures are used to check whether the coordinate of one linkage node is connected to the coordinate of another linkage node in the skeleton image. Each connection between two nodes is a straight linkage.

IV. Numerical Examples

This section shows two different numerical examples to demonstrate the presented methodologies to determine linkage designs automatically.

A. Design Case 1

The setup of the TO design is shown in Fig. 7 where $Lx=16$ in; $Ly=10$ in; thickness of the plate is 1 in; Young's modulus of the material is 2.05×10^5 lb/in^2; Poisson's ratio of the material is 0.3; and the given load F is 3000 lb. Different levels of allowable volume fractions were tested: 70%, 50% and 30%. Fig. 8 shows the results of the volume fraction 70%. Fig. 8 (a) is the TO solution obtained by the solution procedure in section 2. Fig. 8 (b) is the skeleton obtained based on the procedure in sections 3.A and 3.B. The following procedure in section 3.C failed because the differences between the obtained candidates of nodes and the skeleton shown in Fig. 8 (b) were too large to continue.

Fig. 9 shows the results of volume fraction 50%. Fig. 9 (a) and (b) show the TO solution and the obtained skeleton using resolution increment and pattern thinning. Fig. 9 (c) shows the obtained linkage nodes using the presented procedure shown in section 3.3. There are three nodes that are highlighted by red circles cannot be properly located on the skeleton shown in Fig. 9 (b). Therefore, the procedure of generating the linkage design stops at this point.

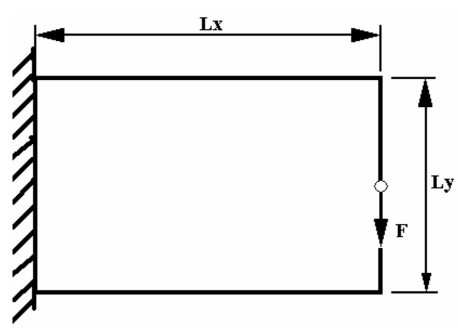

Fig. 7. Conditions of Design Case 1.

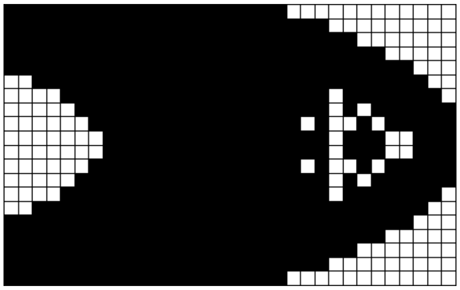
(a)
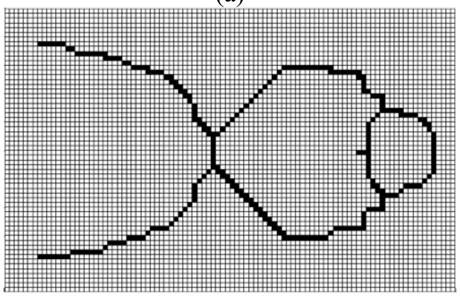
(b)
Fig. 8. Results of Design Case 1 with volume fraction 70%: (a) TO solution, (b) thinning skeleton.

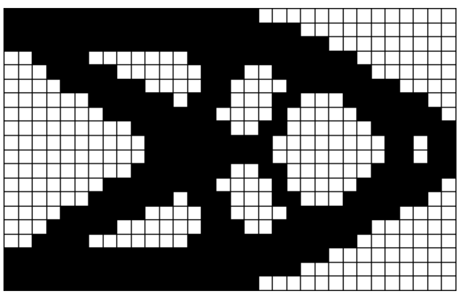
(a)
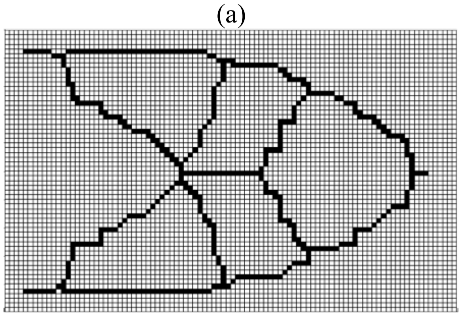
(b)
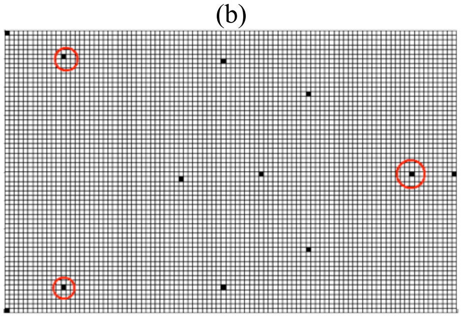
(c)
Fig. 9. Results of Design Case 1 with volume fraction 50%: (a) TO solution, (b) thinning skeleton, (c) obtained linkage nodes.

Fig. 10 shows the results of volume fraction 30%. Fig. 10 (a) shows the TO solution obtained using the procedures in section 2. Fig. 10 (b) shows the obtained skeleton based on the pattern thinning procedure in sections 3.1 and 3.2. Fig. 10 (c) shows the locations of the obtained linkage nodes. In this example, all nodes were properly found and matched to the skeleton sketch in Fig. 10 (b). Finally, a linkage design was successfully generated, as shown in Fig. 10 (d), based on the solution procedures presented in section 3 without any needs of human operations and adjustments. The traditional ways to synthesize a linkage design that satisfies the design objectives and requirements typically require human knowledge and experiences. On the other hand, the proposed methodology based on TO and image processing was able to synthesize a linkage mechanism automatically.

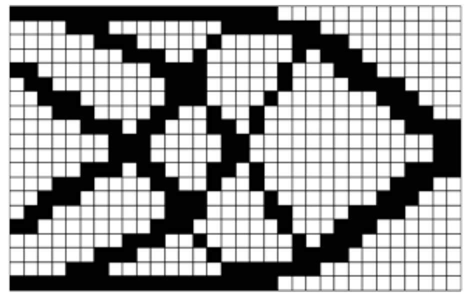
(a)
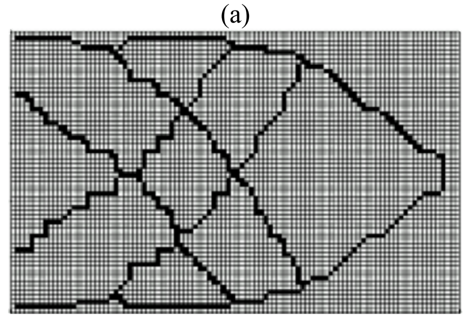
(b)
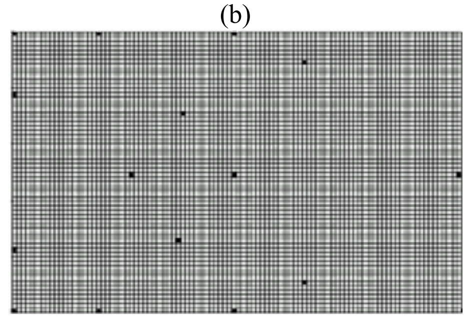
(c)
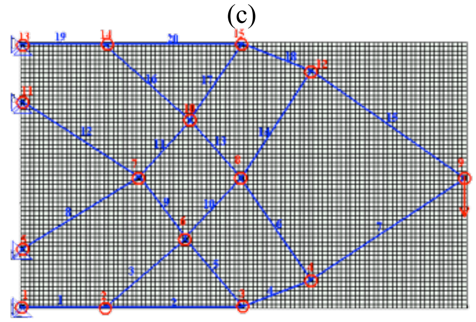
(d)
Fig. 10. Results of Design Case 1 with volume fraction 30%: (a) TO solution, (b) thinning skeleton, (c) obtained linkage nodes, (d) final linkage design.

B. *Design Case 2*

Fig. 11 shows the setup of the second TO design where all parameters are the same as Design Case 1 in section 4.1 but the load is given at a different position. Similarly, three different levels of allowable volume fractions were tested: 70%, 50% and 30%. Similar results were found in the Design Case 2. Fig. 12 shows the TO solution with volume fraction 70% and the obtained skeleton. The linkage nodes could not be determined because they do not match the skeleton sketch in Fig. 12 (b).

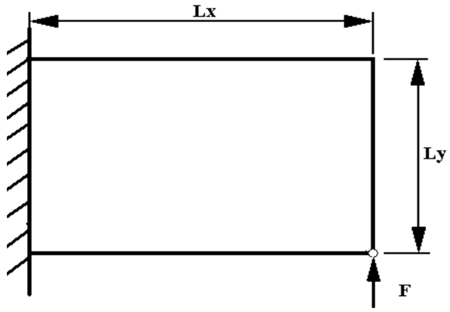

Fig. 11. Conditions of Design Case 2.

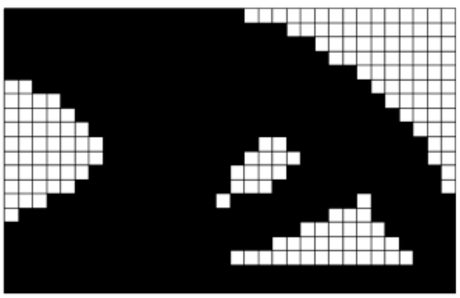

(a)

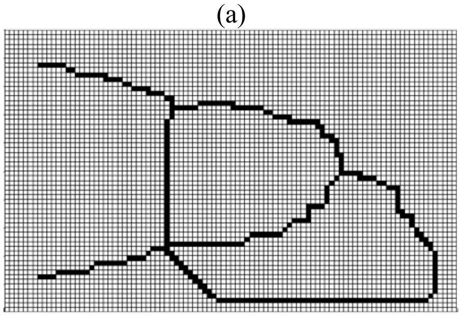

(b)

Fig. 12. Results of Design Case 2 with volume fraction 70%: (a) TO solution, (b) thinning skeleton.

Fig. 13 shows the TO solution of the Design Case 2 with volume fraction 50%. Although the skeleton and the candidates of linkage nodes were determined, as shown in Fig. 13 (b) and (c) respectively, there are three nodes, that are highlighted by red circles do not match the skeleton sketch in Fig. 13 (b). Therefore, the procedure of linkage design stops at this point.

Fig. 14 shows a successful example of automatically generating the linkage design based on TO solution, shown in Fig. 14 (a), and the image processing techniques, that were presented in section 3. Fig. 14 (b) shows the obtained skeleton structure and Fig. 14 (c) shows the obtained positions of linkage nodes. At the end, a linkage design was automatically obtained, as shown in Fig. 14 (d). Similar to the Design Case 1, a new linkage mechanism design was synthesized based on the proposed methodology of TO and image processing without the need of human knowledge and experience. The resultant linkage mechanism would be easy for manufacture and satisfying the design objectives and requirements of the problem.

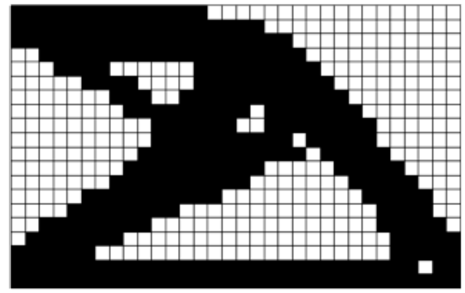

(a)

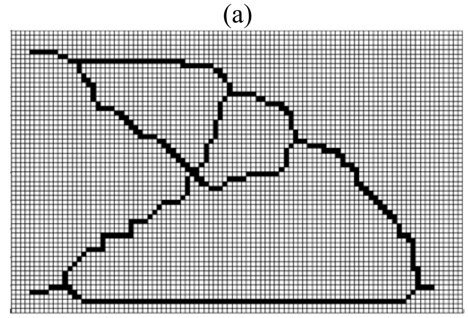

(b)

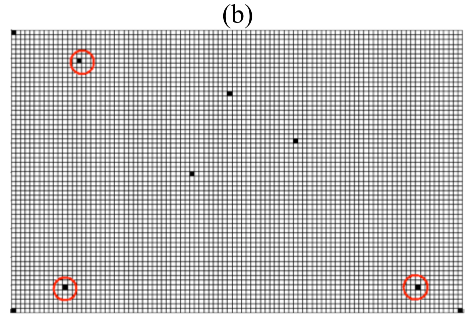

(c)

Fig. 13. Results of Design Case 2 with volume fraction 50%: (a) TO solution, (b) thinning skeleton, (c) obtained linkage nodes.

V. CONCLUSIONS

This paper reviewed some regularization and filtering methods that were used to determine manufacturable topologically optimized structures (i.e. pure black-and-white TO designs). Inspired by the similar processes in the fields of image processing, this paper presents an automatic generation of compliance linkage designs based on TO designs and post-processing of some image processing techniques. The entire procedure starts with the solution process of TO. Thresholding was used to obtain completely black-and-white design. Pattern thinning was then applied to obtain the skeleton of the topologically optimized structure. A series of heuristic rules were used to find the candidates of linkage nodes and match their coordinates in the skeleton sketch. Finally, the linkage design was obtained by linking the nodes that were connected in the skeleton sketch. Two numerical examples with different levels of allowable volume fractions were tested. The results showed that the linkage designs could be automatically generated with proper decisions of design parameters. For practical engineering uses, the generated linkage designs could be optimized by simple shape and size optimizations. The presented automatically generated linkage designs are also suitable for some advanced engineering problems such as structural designs under uncertain loadings [39, 40].

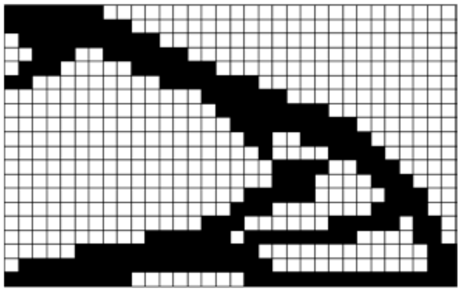

(a)

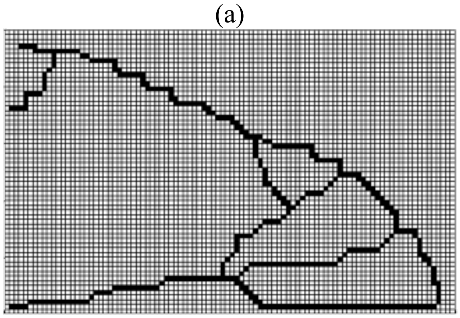

(b)

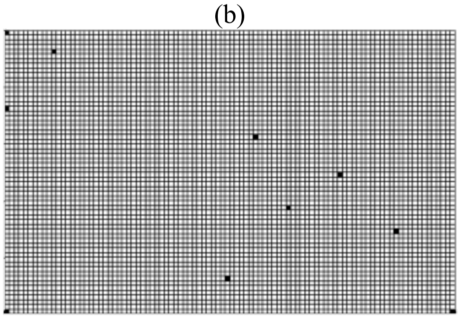

(c)

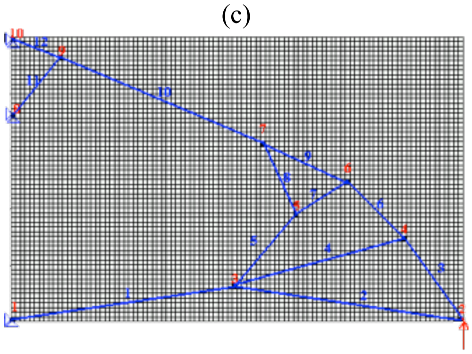

(d)

Fig. 14. Results of Design Case 2 with volume fraction 30%: (a) TO solution, (b) thinning skeleton, (c) obtained linkage nodes, (d) final linkage design.

VI. References

[1] A. G. M. Michell, "LVIII. The limits of economy of material in frame-structures," *The London, Edinburgh, and Dublin Philosophical Magazine and Journal of Science*, vol. 8, no. 47, pp. 589-597, 1904, DOI. 10.1080/14786440409463229.

[2] W. Prager, "Optimality criteria derived from classical extremum principles," *SM Studies Series, Solid Mechanics Division, Univ of Waterloo, Ontario/CANADA*, 1969.

[3] M. P. Bendsøe and N. Kikuchi, "Generating optimal topologies in structural design using a homogenization method," *Computer Methods in Applied Mechanics and Engineering*, vol. 71, no. 2, pp. 197-224, 1988, DOI. 10.1016/0045-7825(88)90086-2.

[4] M. P. Bendsoe, *Optimization of structural topology, shape, and material*, Springer, 1995.

[5] M. C. E. Manuel and P. T. Lin, "Physical-based Material Property Models for Heat Conduction Topology Optimization," presented at the Asian Congress of Structural and Multidisciplinary Optimization, ACSMO 2016, Nagasaki, Japan, 2016.

[6] M. C. E. Manuel and P. T. Lin, "Performance of Alternative Material Property Models for Heat Conduction Topology Optimization," presented at the Asian Congress of Structural and Multidisciplinary Optimization, ACSMO 2016, Nagasaki, Japan, 2016.

[7] M. C. E. Manuel, "A Complete Research on Material Property Models on Heat Conduction Topology Optimization," Thesis, Department of Mechanical Engineering, Chung Yuan Christian University, 2016.

[8] M. C. E. Manuel and P. T. Lin, "Design Explorations of Heat Conductive Pathways," *International Journal of Heat and Mass Transfer*, vol. 104, pp. 835-851, 2017.

[9] M. Stolpe and K. Svanberg, "An alternative interpolation scheme for minimum compliance topology optimization," *Structural and Multidisciplinary Optimization*, vol. 22, no. 2, pp. 116-124, 2001, DOI. 10.1007/s001580100129.

[10] T. E. Bruns, "A reevaluation of the SIMP method with filtering and an alternative formulation for solid–void topology optimization," *Structural and Multidisciplinary Optimization*, vol. 30, no. 6, pp. 428-436, 2005, DOI. 10.1007/s00158-005-0537-x.

[11] R. B. Keey, *Drying: principles and practice*, vol. 13, Elsevier, 2013.

[12] R. L. Hamilton and O. K. Crosser, "Thermal conductivity of heterogeneous two-component systems," *Industrial & Engineering Chemistry Fundamentals*, vol. 1, no. 3, pp. 187-191, 1962.

[13] S. Kirkpatrick, "Percolation and conduction," *Reviews of modern physics*, vol. 45, no. 4, p. 574, 1973, DOI. 10.1103/RevModPhys.45.574.

[14] O. Sigmund, "On the design of compliant mechanisms using topology optimization," *Journal of Structural Mechanics*, vol. 25, no. 4, pp. 493-524, 1997, DOI. 10.1080/08905459708945415.

[15] Z. Luo, L. Tong, M. Y. Wang, and S. Wang, "Shape and topology optimization of compliant mechanisms using a parameterization level set method," *Journal of Computational Physics*, vol. 227, no. 1, pp. 680-705, 2007, DOI. 10.1016/j.jcp.2007.08.011.

[16] M. Jin and X. Zhang, "A new topology optimization method for planar compliant parallel mechanisms," *Mechanism and Machine Theory*, vol. 95, pp. 42-58, 2016, DOI. 10.1016/j.mechmachtheory.2015.08.016.

[17] W. R. Suh, J. M. McCarthy, and E. A. Peraza Hernandez, "Efficient Development of Continuum/Compliant Planar Linkage Mechanisms," presented at the ASME 2019 International Design Engineering Technical Conferences and Computers and Information in Engineering Conference, Anaheim, California, USA, DETC2019-97299, 2019, DOI. 10.1115/DETC2019-97299.

[18] P. Charbonnier, L. Blanc-Féraud, G. Aubert, and M. Barlaud, "Deterministic edge-preserving regularization in computed imaging," *IEEE Transactions on Image Processing*, vol. 6, no. 2, pp. 298-311, 1997, DOI. 10.1109/83.551699.

[19] M. Y. Wang, S. Zhou, and H. Ding, "Nonlinear diffusions in topology optimization," *Structural and Multidisciplinary Optimization*, vol. 28, no. 4, pp. 262-276, 2004, DOI. 10.1007/s00158-004-0436-6.

[20] G. Sapiro, *Geometric partial differential equations and image analysis*, Cambridge university press, 2006.

[21] O. Sigmund, "Morphology-based black and white filters for topology optimization," *Structural and Multidisciplinary Optimization*, vol. 33, no. 4-5, pp. 401-424, 2007, DOI. 10.1007/s00158-006-0087-x.

[22] B. Bourdin, "Filters in topology optimization," *International Journal for Numerical Methods in Engineering*, vol. 50, no. 9, pp. 2143-2158, 2001, DOI. 10.1002/nme.116.

[23] J.-S. Lee, "Digital image enhancement and noise filtering by use of local statistics," *IEEE transactions on pattern analysis and machine intelligence*, no. 2, pp. 165-168, 1980, DOI. 10.1109/TPAMI.1980.4766994.

[24] R. Keys, "Cubic convolution interpolation for digital image processing," *IEEE Transactions on Acoustics, Speech, and Signal Processing*, vol. 29, no. 6, pp. 1153-1160, 1981, DOI. 10.1109/TASSP.1981.1163711.

[25] W. Zhang, W. Zhong, and X. Guo, "An explicit length scale control approach in SIMP-based topology optimization," *Computer Methods in*

Applied Mechanics and Engineering, vol. 282, pp. 71-86, 2014, DOI. 10.1016/j.cma.2014.08.027.
[26] N. Otsu, "A threshold selection method from gray-level histograms," *IEEE Transactions on Systems, Man and Cybernetics*, vol. 9, no. 1, pp. 62-66, 1979.
[27] A. Rosenfeld and L. S. Davis, "A Note on Thinning," *IEEE Transactions on Systems, Man, and Cybernetics*, vol. SMC-6, no. 3, pp. 226-228, 1976, DOI. 10.1109/TSMC.1976.5409243.
[28] M. Bremicker, M. Chirehdast, N. Kikuchi, and P. Papalambros, "Integrated Topology and Shape Optimization in Structural Design," *Journal of Structural Mechanics*, vol. 19, no. 4, pp. 551-587, 1991, DOI. 10.1080/08905459108905156.
[29] O. Sigmund and J. Petersson, "Numerical instabilities in topology optimization: a survey on procedures dealing with checkerboards, mesh-dependencies and local minima," *Structural optimization*, vol. 16, no. 1, pp. 68-75, 1998, DOI. 10.1007/BF01214002.
[30] K. Svanberg, "The method of moving asymptotes- a new method for structural optimization," *International Journal for Numerical Methods in Engineering*, vol. 24, no. 2, pp. 359-373, 1987, DOI. 10.1002/nme.1620240207.
[31] O. Sigmund, "A 99 line topology optimization code written in Matlab," *Structural and Multidisciplinary Optimization*, vol. 21, no. 2, pp. 120-127, 2001, DOI. 10.1007/s001580050176.
[32] E. Andreassen, A. Clausen, M. Schevenels, B. S. Lazarov, and O. Sigmund, "Efficient topology optimization in MATLAB using 88 lines of code," *Structural and Multidisciplinary Optimization*, vol. 43, no. 1, pp. 1-16, 2011, DOI. 10.1007/s00158-010-0594-7.
[33] K. Liu and A. Tovar, "An efficient 3D topology optimization code written in Matlab," *Structural and Multidisciplinary Optimization*, vol. 50, no. 6, pp. 1175-1196, 2014, DOI. 10.1007/s00158-014-1107-x.
[34] S. Jin, J. Kim, J. Bae, T. Seo, and J. Kim, "Design, modeling and optimization of an underwater manipulator with four-bar mechanism and compliant linkage," *Journal of mechanical science and technology*, vol. 30, no. 9, pp. 4337-4343, 2016.
[35] D. Fedorov and L. Birglen, "Design of a self-adaptive robotic leg using a triggered compliant element," *IEEE Robotics and Automation Letters*, vol. 2, no. 3, pp. 1444-1451, 2017.
[36] Y. She, H.-J. Su, D. Meng, and C. Lai, "Design and Modeling of a Continuously Tunable Stiffness Arm for Safe Physical Human–Robot Interaction," *Journal of Mechanisms and Robotics*, vol. 12, no. 1, 2020.
[37] Y.-J. Kim, H. Song, and C.-Y. Maeng, "BLT Gripper: An Adaptive Gripper with Active Transition Capability between Precise Pinch and Compliant Grasp," *IEEE Robotics and Automation Letters*, 2020.
[38] T. Pavlidis, "A thinning algorithm for discrete binary images," *Computer graphics and image processing*, vol. 13, no. 2, pp. 142-157, 1980, DOI. 10.1016/S0146-664X(80)80037-2.
[39] J. Liu, H. C. Gea, and P. A. Du, "Robust Structural Design Optimization Under Non-Probabilistic Uncertainties," presented at the ASME 2011 International Design Engineering Technical Conferences and Computers and Information in Engineering Conference, Washington, DC, USA, DETC2011-48710, 2011, DOI. 10.1115/DETC2011-48710.
[40] J. Liu and H. C. Gea, "Robust topology optimization under multiple independent unknown-but-bounded loads," *Computer Methods in Applied Mechanics and Engineering*, vol. 329, pp. 464-479, 2018, DOI. 10.1016/j.cma.2017.09.033.

Po Ting Lin received the M.S. and Ph.D. degrees in the Department of Mechanical and Aerospace Engineering from Rutgers University, New Brunswick, New Jersey, USA in 2007 and 2010, respectively. He is currently an Associate Professor in the Department of Mechanical Engineering, National Taiwan University of Science and Technology, Taipei, Taiwan. His current research interests and publications are in the areas of Machine Vision, Robotics, Machine Learning, Reliability-Based Design Optimization, and Multidisciplinary Design Optimization

Chyi-Yeu Lin received the M.S. degree in the Department of Mechanical Engineering from Tamkang University, New Taipei City, Taiwan in 1985 and received the Ph.D. degree in the Department of Aerospace Engineering, Mechanics and Engineering Science from University of Florida, Florida, USA in 1991. He is currently a Distinguished Professor in the Department of Mechanical Engineering and the Director of Center for Intelligent Robots at National Taiwan University of Science and Technology, Taipei, Taiwan. His current research interests and publications are in the areas of Intelligent Robots, Intelligent Machines, Computer Vision, Artificial Intelligence, Optimal Design, and Structural Optimization.

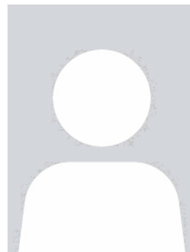

Tung-Yao Cheng received the M.S. degree in the Department of Mechanical Engineering, National Taiwan University of Science and Technology, Taipei, Taiwan in July 2005.